

# Gaussian boson sampling with partial distinguishability

Junheng Shi<sup>1, 2</sup> and Tim Byrnes<sup>2, 3, 1, 4, 5, \*</sup>

<sup>1</sup>*State Key Laboratory of Precision Spectroscopy, School of Physical and Material Sciences, East China Normal University, Shanghai 200062, China*

<sup>2</sup>*New York University Shanghai, 1555 Century Ave, Pudong, Shanghai 200122, China*

<sup>3</sup>*NYU-ECNU Institute of Physics at NYU Shanghai, 3663 Zhongshan Road North, Shanghai 200062, China*

<sup>4</sup>*National Institute of Informatics, 2-1-2 Hitotsubashi, Chiyoda-ku, Tokyo 101-8430, Japan*

<sup>5</sup>*Department of Physics, New York University, New York, New York 10003, USA*

(Dated: May 20, 2021)

Gaussian boson sampling (GBS) allows for a way to demonstrate quantum supremacy with the relatively modest experimental resources of squeezed light sources, linear optics, and photon detection. In a realistic experimental setting, numerous effects can modify the complexity of the sampling, in particular loss, partial distinguishability of the photons, and the use of threshold detectors rather than photon counting detectors. In this paper, we investigate GBS with partial distinguishability by introducing the concepts of virtual modes and indistinguishability efficiency. We develop a model based on these concepts and derive the probabilities of measuring a specific output pattern from partially distinguishable and lossy GBS for both types of detectors. In the case of threshold detectors, the probability as calculated by the Torontonian is a special case under our framework. By analyzing the expressions of these probabilities we propose an efficient classical simulation algorithm which can not only be used to calculate the probabilities, but also provides a foundation for an approximation method that decreases the computational time exponentially. Using this approximation we show how partial distinguishability affects quantum supremacy by GBS.

## I. INTRODUCTION

It is commonly believed that quantum computers have the ability to outperform classical computers and falsify the Extended Church-Turing Thesis [1]. In order to demonstrate this quantum speedup, one requires not only a large number of qubits but also sufficiently suppressed logical errors. Decoherence typically removes the quantum aspect of the computation, such that it becomes possible to classically simulate the computation efficiently. Specifically, quantum supremacy is claimed when the quantum device achieves a superpolynomial quantum speedup. This was the case in the comparison between the quantum processor created by Martinis and co-workers [2] and the counter-classical simulation algorithms of Ref. [3] and recently from Ref. [4].

Another heated battlefield in the context of quantum supremacy is the boson sampling (BS) problem where a passive linear optics interferometer, Fock states at the input, and photon-detectors are placed at the output. It was proved by Aaronson & Arkhipov [1] that the output distribution of such device cannot be efficiently simulated by a classical computer in polynomial time [5, 6] because it corresponds to the permanent of a given transformation matrix. However, challenges arise in the experimental implementation Aaronson & Arkhipov's boson sampling (AABS). One of them is the low generation efficiency of single photons. To truly outperform the state-of-art classical simulation algorithm for AABS [7], at least 50 photons are required at the input. But due

to the low single photon efficiency of solid state sources [8–10] which is typically between 0.2 and 0.3, the largest experimentally demonstrated number of single photon inputs in AABS has only been 20 to date [11]. It was then proposed that this challenge can be tackled by changing the input light from Fock states to Gaussian states which was first conceived in the form of Scattershot Boson Sampling (SBS) [12, 13] and later developed to GBS [14, 15]. The probability of measuring a specific output pattern in GBS corresponds to the Hafnian of a matrix [16] which has been also proven as being computationally hard [5]. While generally the significance of BS is in relation to quantum supremacy, GBS has also potential applications in finding subgraphs [17] and molecular vibronic spectra [18].

GBS was first realized in small-scale experiments [19, 20]. Recently quantum supremacy was claimed in a GBS experiment by Pan, Lu, and co-workers [21] which was able to generate up to 76 photon detection events at the output of a 100-mode interferometer. It should be noted the average output photon detection events is in the vicinity of 40 which means that it was not in the collision-free regime which most of the current GBS theories fall into. Another major aspect of the experiment is the type of detection device used. In the experiment, threshold detectors, rather than photon number resolving (PNR) detectors were used, which only indicate the presence or lack of a photon. The use of threshold detectors changes the underlying theory because the output probability distributions is no longer determined by a Hafnian, but the Torontonian of the matrix representing the linear optical network [22, 23]. These two matrix functions have the same computational complexity for

\* corresponding author: tim.byrnes@nyu.edu

the ideal case which is  $O(N^3 2^N)$  for a  $2N \times 2N$  matrix. Despite this, the origin of the complexity is rather different for the two cases. In the case of the Hafnian, the complexity arises due to the large number of permutations of matrix elements; meanwhile the complexity of computing Torontonian comes from the computation of  $2^N$  determinants.

Another major challenge is to understand the impact of experimental imperfections such as losses [24, 25], network noise [26] and partial photon distinguishability [27–31]. Similarly to AABS, the original theory of GBS only handles the ideal case and is not easily extendable to include these imperfections. So far, only losses and detector dark counts in GBS have been analyzed [32]. Ref. [32] is based on the framework of Ref. [24] where the generalized Wigner function is used to demarcate the region of efficient classical simulation as a function of losses and detector dark counts. In contrast, no analysis has been carried out for partial photon distinguishability in GBS, except for a recent paper [33] claiming to extend their results for partial distinguishability in AABS to that in GBS. The results of Ref. [33] are somewhat unsatisfactory in the sense that their results for GBS must be applied in a context similar to AABS. For example, their investigation is strictly limited to the collision-free regime with weak squeezing, and they presume that the number of photons generated by the source is fixed and known at the beginning of the derivation. This is a rather strong assumption in relation to the indeterminate photon number nature of Gaussian states, especially in the presence of loss. In addition, Ref. [33] only discusses GBS with PNR detectors, such that the theory is not applicable to the current GBS experiments using threshold detectors.

In this paper, we provide an investigation of the partial distinguishability problem in GBS, not limited by the collision-free or determinate photon number assumptions. We develop a model for partial distinguishability and apply it to GBS with both PNR and threshold detectors. In this model we introduce a new parameter called the indistinguishability efficiency. Along with other existing parameters such as the squeezing parameter of the input light and transmission rate introduced from the lossy GBS model, it forms composite parameters that affect the probability distribution and its underlying structure, similar to how transmission rate and dark counts work together to determine the classical simulability of imperfect AABS [24]. We define virtual modes to incorporate the distinguishable photons that do not interfere with other photons but contribute to the photon detection at the end. For GBS with PNR detectors, the resulting probability is calculated as a sum of all possible combinations of different outputs of these states. Despite starting from completely different models, we find our characterization of the distinguishable photons in GBS matches perfectly with that derived for AABS [34], which adds evidence towards the validity of our model. For GBS with threshold detectors, we include both partial distinguishability and losses in deriving the

expression for the probability. We note that previous works are limited to ideal GBS. In order to include the distinguishable photons from the virtual modes, we abandon the commonly employed Torontonian method and propose a new method based on the marginal probability and prove that the probability defined by Torontonian is a special case of our result.

We finally discuss how partial distinguishability affects the quantum supremacy in light of our result. For partially distinguishable GBS with PNR detectors, since every term in the output probability corresponds to a particular number of indistinguishable photons, this determines the computational cost of calculating that term. By showing that the cost increases exponentially with the number of indistinguishable photons, we obtain an approximation by considering only a fraction of all terms which involves a smaller number of indistinguishable photons; in other words, it becomes more “classical”. We check the fidelity of the approximation which depends mainly on the indistinguishability efficiency. For a given fidelity, our approximation takes less computational time than ideal GBS and decreases exponentially with reducing indistinguishability efficiency. In this way, we show that partial distinguishability affects quantum supremacy.

## II. THE MODEL OF PARTIAL DISTINGUISHABILITY

A typical GBS scheme consists of three parts: an interferometer with  $K$  spatial ports for inputting photons and  $K$  ports for outputs;  $M$  of these input ports are fed with squeezed vacuum states and each output port has a detector. We note that what we refer to as “ports” are commonly referred to as “modes” in most of the literature on boson sampling since all photons are typically assumed to be indistinguishable. In this paper, we use the word “port” since each port may consist of multiple modes. The interferometer is characterized by a  $K \times K$  Haar random matrix  $\mathbf{T}$  where its columns correspond to the input ports and its rows correspond to the output ports.

It is convenient to represent a Gaussian state by a quasiprobability distribution (QPD) because the first two statistical moments of the QPD — the displacement vector and covariance matrix — are sufficient to fully characterize the density matrix [35, 36]. Since the Gaussian states we are dealing with always have zero displacement vector, we write  $\rho = \rho(\mathbf{V})$  and only use the covariance matrix  $\mathbf{V}$  to represent the density matrix. Its definition is given by

$$V_{kl} = \frac{1}{2} \langle \{\Delta \hat{\mathbf{x}}_k, \Delta \hat{\mathbf{x}}_l\} \rangle, \quad (1)$$

where  $\Delta \hat{\mathbf{x}} = \hat{\mathbf{x}} - \langle \hat{\mathbf{x}} \rangle$  and the quadrature field operators are defined as  $\hat{\mathbf{x}} = [\hat{q}_1, \hat{p}_1, \dots, \hat{q}_K, \hat{p}_K]$ ,  $\hat{q}_k = \hat{a}_k + \hat{a}_k^\dagger$ ,  $\hat{p}_k =$

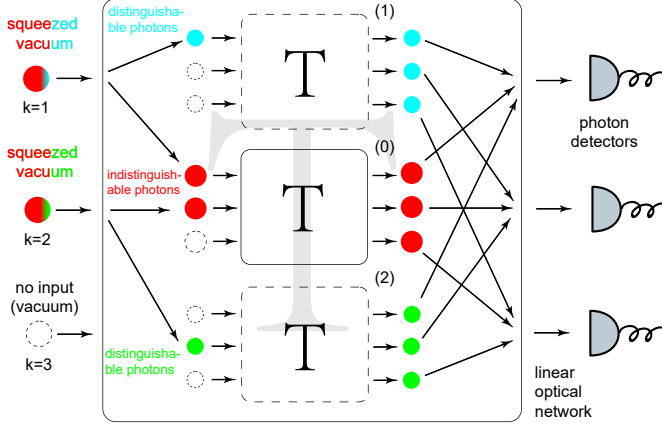


FIG. 1. A pictorial representation of our model. For the simplicity of illustration, we show a  $3 \times 3$  interferometer ( $K=3$ ) characterized by  $\mathbf{T}$  with input light at first two ports ( $M=2$ ). When partially distinguishable input light (represented by the mixed color ball for the input ports) enters the interferometer, they decompose into non-interfering modes and propagate inside the interferometer independently until they leave the interferometer and collectively meet the detectors at the output ports. The thin solid-lined rectangle represents the interferometer for the indistinguishable photons. The dashed rectangles represent the interferometer for the distinguishable virtual modes.

$i(\hat{a}_k^\dagger - \hat{a}_k)$ , and  $\hat{a}_k$  are the annihilation operators for the  $k$ th port. We let  $k \in [1, K]$  throughout the paper.

By directly using the existing model for lossy GBS as in Ref. [32], the covariance matrix of squeezed vacuum inputs with losses is

$$\mathbf{V}^{(0)} = \bigoplus_{m=1}^M \begin{bmatrix} \eta_t e^{2r_m} + 1 - \eta_t & 0 \\ 0 & \eta_t e^{-2r_m} + 1 - \eta_t \end{bmatrix} \bigoplus \mathbf{I}_{2K-2M} \quad (2)$$

where  $\eta_t$  is the overall transmission rate:

$$\eta_t = \eta_s \eta_u \eta_d. \quad (3)$$

Here,  $\eta_s$  is the transmission of the inputs (sources) before entering the interferometer,  $\eta_u$  is the transmission for the uniform loss inside the interferometer, and  $\eta_d$  is the detection efficiency. In principle, we should only include  $\eta_s$  in Eq.(2) because it describes the Gaussian state before entering the interferometer, but since our model is compatible with the result in Ref. [7, 32], we combine  $\eta_s$ ,  $\eta_u$  and  $\eta_d$  at this stage. Here,  $\mathbf{I}_n$  is the  $n \times n$  identity matrix which is the covariance matrix of the vacuum state. A standard assumption that is typically used in experiments such as Ref. [21] is that all inputs have identical squeezing parameter  $r_m = r$ . The superscript  $(0)$  is used to denote the quantities and parameters related to the indistinguishable photons.

For GBS, partial distinguishability originates from imperfect input light where minor shifts in time or frequency is the origin of the distinguishability [30, 31]. To

characterize it, in our model all input light is initially indistinguishable. Before entering the interferometer, they go through a process where each photon has the probability of becoming a distinguishable photon. These photons do not interfere with other photons during their propagation in the interferometer, but will be registered by the detectors at the output. In order to satisfy this assumption, we create an additional virtual mode for every port which has input light. The Gaussian state in each virtual mode is characterized as  $\rho^{(m)}(\mathbf{V}^{(m)})$ . Throughout the paper, the superscript  $(m)$  is used to denote the quantities and parameters related to the distinguishable photons in the  $m$ th virtual mode and we let  $m \in [1, M]$ , while  $m' \in [0, M]$  which includes the indistinguishable mode  $m' = 0$ . These virtual modes are initially in vacuum states,  $\mathbf{V}^{(m)} = \mathbf{I}_{2K}$ , until they are fed with photons through the corresponding port from the indistinguishable mode. The transformation of photons from the indistinguishable mode to the virtual modes is characterized by the unitary operator:

$$U_m = \exp \left\{ \theta (\hat{a}_m^\dagger \hat{b}_m^{(m)} - \hat{b}_m^{(m)\dagger} \hat{a}_m) \right\}, \quad (4)$$

where  $\hat{a}_m^\dagger$  and  $\hat{a}_m$  are the creation and annihilation operators of the  $m$ th port of the indistinguishable mode,  $\hat{b}_m^{(m)\dagger}$  and  $\hat{b}_m^{(m)}$  are the creation and annihilation operators of the  $m$ th port of the  $m$ th virtual mode. Here, the subscript  $m$  is to indicate which port. We define the indistinguishability efficiency as the probability of a photon not exchanged from the indistinguishable mode to the virtual modes, denoted as  $\eta_{\text{ind}}$ . Under the effect of Eq.(4), it satisfies the relation:

$$\eta_{\text{ind}} = \cos^2 \theta. \quad (5)$$

There is some similarity between this model and that for lossy GBS [24, 32], but the major difference is that the photons in the virtual modes are not lost, instead, they go on to propagate in the interferometer until they are detected at the output.

Now we obtain the new density matrices for all  $M+1$  modes after applying the distinguishable-indistinguishable transformation by taking the partial trace:

$$\tilde{\rho} = \left( \prod_{m=1}^M U_m \right) \bigotimes_{m'=0}^M \rho^{(m')} \left( \prod_{m=1}^M U_m \right)^\dagger \quad (6)$$

$$\tilde{\rho}^{(m')} = \text{tr}_{m'}(\tilde{\rho}). \quad (7)$$

Since we use the covariance matrix to represent the density matrix, we give the covariance matrices of all  $M+1$  modes:

$$\tilde{\mathbf{V}}^{(0)} = \bigoplus_{m=1}^M \begin{bmatrix} \mathcal{X}_{\text{ind}} & 0 \\ 0 & \mathcal{Y}_{\text{ind}} \end{bmatrix} \bigoplus \mathbf{I}_{2K-2M} \quad (8)$$

$$\tilde{\mathbf{V}}^{(m)} = \mathbf{I}_{2m-2} \bigoplus \begin{bmatrix} \mathcal{X}_{\text{dis}} & 0 \\ 0 & \mathcal{Y}_{\text{dis}} \end{bmatrix} \bigoplus \mathbf{I}_{2K-2m}, \quad (9)$$

where we have

$$\mathcal{X}_{\text{ind}} = \eta_t \eta_{\text{ind}} e^{2r} + 1 - \eta_t \eta_{\text{ind}} \quad (10)$$

$$\mathcal{Y}_{\text{ind}} = \eta_t \eta_{\text{ind}} e^{-2r} + 1 - \eta_t \eta_{\text{ind}} \quad (11)$$

$$\mathcal{X}_{\text{dis}} = \eta_t (1 - \eta_{\text{ind}}) e^{2r} + 1 - \eta_t (1 - \eta_{\text{ind}}) \quad (12)$$

$$\mathcal{Y}_{\text{dis}} = \eta_t (1 - \eta_{\text{ind}}) e^{-2r} + 1 - \eta_t (1 - \eta_{\text{ind}}). \quad (13)$$

In our model, the output pattern measured at detection does not only come from the indistinguishable mode. It is the combined output pattern of all  $M+1$  modes. Consider the case of ideal PNR detection. If the output pattern of the  $m'$ th mode is  $\mathbf{s}^{(m')} = [s_1^{(m')}, s_2^{(m')}, \dots, s_K^{(m')}]$  where  $s_k^{(m')}$  denotes the number of output photons at  $k$ th port of  $m'$ th mode, then the overall output pattern is

$$\mathbf{s} = \sum_{m'=0}^M \mathbf{s}^{(m')}, \quad (14)$$

and for each port we have

$$s_k = \sum_{m'=0}^M s_k^{(m')}. \quad (15)$$

### III. PARTIALLY DISTINGUISHABLE GAUSSIAN BOSON SAMPLING WITH PNR DETECTORS

We now proceed to calculate the probability distribution of the output for PNR detectors. For the original GBS with perfect indistinguishability, the probability of observing an output pattern  $\mathbf{s} = [s_1, s_2, \dots, s_K]$  where  $s_k$  is the number of detected photons at the output of the  $k$ th port is given by the equation:

$$P(\mathbf{s}) = \frac{\text{Haf}(\mathbf{A}_{\mathbf{s}})}{s_1! \dots s_K! \sqrt{\det(\mathbf{Q})}}, \quad (16)$$

where  $\text{Haf}(\cdot)$  stands for the matrix function Hafnian and  $\mathbf{A}_{\mathbf{s}}$  is the selected kernel matrix which is obtained by repeating rows and columns of the kernel matrix according to  $\mathbf{s}$ . The kernel matrix is constructed out of the covariance matrix.  $\mathbf{Q}$  is the covariance matrix of Q-function [37].

For partially distinguishable GBS under our model, we need to first decompose the overall output pattern into different combinations of  $M+1$  patterns, namely  $\mathbf{s}^{(0)}, \mathbf{s}^{(1)} \dots \mathbf{s}^{(M)}$ , according to Eq.(14) and Eq.(15). We define  $P^{(m')}(\mathbf{s}^{(m')})$  as the probability to obtain output pattern  $\mathbf{s}^{(m')}$  for the  $m'$ th mode. The probabilities of all possible combinations are then combined to obtain the overall probability:

$$P(\mathbf{s}) = \sum_{\mathbf{s}^{(0)}} \sum_{\mathbf{s}^{(1)}} \dots \sum_{\mathbf{s}^{(M)}} \prod_{m'=0}^M P^{(m')}(\mathbf{s}^{(m')}), \quad (17)$$

where the  $\mathbf{s}$  is defined as in Eq.(14).

In Eq.(17) there are a total of  $\prod_{k=1}^K (s_k^{(0)} + 1)$  possible configurations of  $\mathbf{s}^{(0)}$ , ranging from  $[0, \dots, 0]$  to  $[s_1, \dots, s_K]$ . Now we regroup them by the total number of photons in a configuration, denoted as  $N^{(0)}$ :

$$N^{(0)} = \sum_{k=1}^K s_k^{(0)}, \quad (18)$$

and rewrite Eq.(17) as

$$P(\mathbf{s}) = \sum_{n=0}^N \sum_{\substack{\mathbf{s}^{(0)} \\ \{N^{(0)}=n\}}} P^{(0)}(\mathbf{s}^{(0)}) P_{\text{dis}}(\mathbf{s} - \mathbf{s}^{(0)}), \quad (19)$$

where

$$P_{\text{dis}}(\mathbf{s}_{\text{dis}}) = \sum_{\substack{\mathbf{s}^{(1)}, \dots, \mathbf{s}^{(M)} \\ \{\sum_{m=1}^M s^{(m)} = \mathbf{s}_{\text{dis}}\}}} \prod_{m=1}^M P^{(m)}(\mathbf{s}^{(m)}), \quad (20)$$

where  $N$  is the total number of photons of the overall output pattern:

$$N = \sum_{k=1}^K s_k. \quad (21)$$

Here, we consider the photons from all the virtual modes as a whole because later we propose an classical sampling algorithm for their combined probability in Eq.(20).

In Appendix A, we obtain the covariance matrix  $\mathbf{Q}$  and kernel matrix  $\mathbf{A}$  of all  $M+1$  modes. Applying them to Eq.(16) we obtain the specific probability distribution for each state. The expression for the probability with respect to the indistinguishable mode takes the same form as Eq.(16):

$$P^{(0)}(\mathbf{s}^{(0)}) = \frac{\text{Haf}(\mathbf{A}_{\mathbf{s}^{(0)}})}{s_1^{(0)}! \dots s_K^{(0)}! \sqrt{\det(\mathbf{Q}^{(0)})}}. \quad (22)$$

For the distinguishable modes, on the other hand, the change in the form of kernel matrix leads to the reduction of the Hafnian matrix function to simple multiplication:

$$P^{(m)}(\mathbf{s}^{(m)}) = \frac{G(N^{(m)})}{\sqrt{\det(\mathbf{Q}^{(m)})}} \prod_{k=1}^K \frac{|T_{k,m}|^{2s_k^{(m)}}}{s_k^{(m)}!}, \quad (23)$$

$$G(N^{(m)}) = \sum_q \frac{(N^{(m)}!)^2}{(q!!)^2 (N^{(m)} - q)!} \beta_d'^q \alpha_d'^{N^{(m)} - q}, \quad (24)$$

where  $q \in \{0, 2, \dots, 2 \lfloor \frac{N^{(m)}}{2} \rfloor\}$  and  $N^{(m)}$  is the total number of photons in the  $m$ th virtual mode

$$N^{(m)} = \sum_{k=1}^K s_k^{(m)}. \quad (25)$$

Here,  $T_{k,m}$  is an element of the interferometer matrix  $\mathbf{T}$ . It represents the amplitudes of the transformation of a photon from the  $m$ th port to the  $k$ th port. Expressions for parameters  $\beta'_d$  and  $\alpha'_d$  are

$$\alpha'_d = \frac{\eta_t(1 - \eta_{\text{ind}})(1 - \eta_t(1 - \eta_{\text{ind}})) \sinh^2 r}{1 + \eta_t(1 - \eta_{\text{ind}})(2 - \eta_t(1 - \eta_{\text{ind}})) \sinh^2 r}, \quad (26)$$

$$\beta'_d = \frac{\eta_t(1 - \eta_{\text{ind}}) \sinh r \cosh r}{1 + \eta_t(1 - \eta_{\text{ind}})(2 - \eta_t(1 - \eta_{\text{ind}})) \sinh^2 r}. \quad (27)$$

A detailed derivation of Eq.(23) can be found in Appendix B. Hence the computational complexity of calculating one specific probability from  $m$ th virtual mode is only a 1st degree polynomial respect to total number of output photons.

It should be noted that this result does not indicate that the exact calculation of  $P_{\text{dis}}$  can be done in polynomial time, because it contains  $\prod_{k=1}^K \frac{(M-1+s_k)!}{(M-1)!s_k!}$  terms. Each term corresponds to a possible combination of  $\mathbf{s}^{(1)}, \dots, \mathbf{s}^{(M)}$ . For the extreme case of the collision-free regime, there would still be  $M^N$  terms. Even though the computational complexity of calculating each term is only polynomial according to Eq.(23), adding them costs at least exponential time. Nevertheless, unlike Eq.(22), Eq.(23) provides a back door for classical simulation. In the next section we propose an classical simulation method for generating  $P_{\text{dis}}$ .

#### IV. EFFICIENT CLASSICAL SIMULATION FOR DISTINGUISHABLE GAUSSIAN BOSON SAMPLING

Looking at Eq.(23) closely, we find that by multiplying an additional factorial, the product on the right side forms a multinomial distribution:

$$P_{\text{prod}}^{(m)}(\mathbf{s}) = N! \prod_{k=1}^K \frac{|T_{k,m}|^{2s_k}}{s_k!}, \quad (28)$$

which means that the output port of each photon is randomly chosen among all  $K$  ports following the probability distribution  $(|T_{1,m}|^2, |T_{2,m}|^2, \dots, |T_{K,m}|^2)$ .  $P_{\text{prod}}^{(m)}(\mathbf{s})$  is also related to the probability distribution of obtaining output pattern  $\mathbf{s}$  in distinguishable AABS [34]:

$$P_{\text{AA}}(\mathbf{s}) = \frac{\text{Perm}(\mathbf{T}_s^\#)}{s_1! \dots s_K!}, \quad (29)$$

where  $\mathbf{T}_s^\#$  denotes a matrix with entries  $|T_{ij}|^2$  where  $T_{ij}$  is an entry of the original complex AABS transformation matrix  $\mathbf{T}_s$ . Under the condition that there is only one input port, Eq.(29) reduces to Eq.(28). With this in mind, the remaining coefficients in Eq.(23) can be interpreted as the probability of obtaining  $N^{(m)}$  photons from the state described by Eq.(9):

$$P_{\text{num}}^{(m)}(N) = \frac{G(N)}{N! \sqrt{\det(\mathbf{Q}^{(m)})}}. \quad (30)$$

Now we can write Eq.(23) as a multiplication of Eq.(28) and Eq.(30).

Such an analysis enables us to provide a classical sampling method for distinguishable GBS, with the help of the two probabilities distributions  $P_{\text{prod}}^{(m)}(\mathbf{s})$  and  $P_{\text{num}}^{(m)}(N)$ . Before doing that, we need to set the range for the number of photons. Theoretically, this range is from zero to infinity, but since the probability decreases exponentially with  $N$ , since  $G(N) \propto \alpha_d^N$ , it is convenient to truncate the sampling range at a number,  $N_t = \bar{N}_d t$  where  $\bar{N}_d$  is the average number of photons:

$$\bar{N}_d = \eta_t(1 - \eta_{\text{ind}}) \sinh^2 r, \quad (31)$$

and  $t$  is a truncation factor. Due to the truncation we renormalize  $P_{\text{num}}^{(m)}(N)$  according to:

$$\tilde{P}_{\text{num}}^{(m)}(N) = \frac{P_{\text{num}}^{(m)}(N)}{\sum_{n=1}^{N_t} P_{\text{num}}^{(m)}(n)}. \quad (32)$$

---

#### Algorithm 1: Efficient sampling of distinguishable GBS

---

```

input :  $M, K, N$ , an  $K \times K$  matrix  $\mathbf{T}$  and  $M$  pmfs
       $\tilde{\mathbf{P}}_{\text{num}}^{(m)} = (\tilde{P}_{\text{num}}^{(m)}(0), \dots, \tilde{P}_{\text{num}}^{(m)}(N))$ 
output: a sample  $\mathbf{s}$ 

1  $\mathbf{s} \leftarrow (s_1, \dots, s_K)$  ;
2  $s_1 \leftarrow \dots \leftarrow s_K \leftarrow 0$ ;
3 for  $m \leftarrow 1$  to  $M$  do
4    $N^{(m)} \leftarrow \text{Sample}(\tilde{\mathbf{P}}_{\text{num}}^{(m)})$ ; // Sample a  $N^{(m)}$  from
     $(0, 1, \dots, N)$  with pmf  $\tilde{\mathbf{P}}_{\text{num}}^{(m)}$ 
5    $\mathbf{w}_m \leftarrow (|T_{1,m}|^2, \dots, |T_{K,m}|^2)$ ;
6   for  $i \leftarrow 1$  to  $N^{(m)}$  do
7      $j \leftarrow \text{Sample}(\mathbf{w}_m)$ ; // Sample a  $j$  from
       $(1, \dots, K)$  with pmf  $\mathbf{w}_m$ 
8      $s_j \leftarrow s_j + 1$ ;
9   end
10 end
11 return  $\mathbf{s}$ 

```

---

Algorithm 1 then allows us to sample the output pattern from all virtual modes. The computational complexity of the worst-case scenario is  $O(MK \lceil t\alpha_d \rceil)$  which is only polynomial. We can create a probability distribution of all output patterns from distinguishable GBS with  $\varepsilon$  accuracy requiring a computational cost  $O(MK \lceil t\alpha_d \rceil / \varepsilon)$ .  $n$  binary digit accuracy can be achieved for each probability if we let  $\varepsilon = 1/2^n$ . We denote this probability distribution as  $P_{\text{sim}}(\mathbf{s}, \varepsilon)$ .

While  $P_{\text{dis}}(\mathbf{s})$  is only calculated one individual  $\mathbf{s}$  at a time,  $P_{\text{sim}}(\mathbf{s}, \varepsilon)$  updates the probabilities for all output patterns simultaneously with each sampling. This is extremely useful in Eq.(19) where  $P_{\text{dis}}(\mathbf{s})$  of a considerable number of different patterns  $\mathbf{s}$  needs to be calculated to obtain the result. Naturally we obtain an approximation to  $P(\mathbf{s})$  with accuracy  $\varepsilon$  by replacing  $P_{\text{dis}}(\mathbf{s})$  with  $P_{\text{sim}}(\mathbf{s}, \varepsilon)$ .

## V. PARTIALLY DISTINGUISHABLE GAUSSIAN BOSON SAMPLING WITH THRESHOLD DETECTORS

In the original proposal of GBS, each output port has a PNR detector. For a quantum supremacy demonstration, the number of ports — and hence the number of PNR detectors — is rather large, which may be prohibitive experimentally. As such, in works such as Ref. [21] they were replaced with threshold detectors where the detection result only shows the presence of the photons regardless of its exact number. If any number of photons greater or equal to one are detected, it is referred to as a “click”. Of course, the probability of a click can be calculated by adding up the probabilities of all possible output patterns from PNR detectors over an infinite number of terms. A better way than this direct approach is to use the P-functions of the POVM elements  $|0\rangle\langle 0|$  and  $\hat{\mathbf{I}} - |0\rangle\langle 0|$ , where one can directly calculate the probability of the output pattern  $\mathbf{s}$  as in Ref. [22]

$$P(\mathbf{s}) = \frac{\text{Tor}(\mathbf{Q}_{\mathcal{U}})}{\sqrt{\det(\mathbf{Q})}}, \quad (33)$$

with a matrix function defined as Torontonian:

$$\text{Tor}(\mathbf{Q}_{\mathcal{U}}) = \sum_{\mathcal{V} \in \mathcal{P}(\mathcal{U})} (-1)^{|\mathcal{U}| - |\mathcal{V}|} \frac{1}{\sqrt{\det((\mathbf{Q}^{-1})_{\mathcal{V}})}}. \quad (34)$$

Here,  $\mathcal{U}$  is a set where the elements are the ports that have clicks in pattern  $\mathbf{s}$ ,  $\mathcal{P}(\mathcal{U})$  is the power set which contains all the subsets of  $\mathcal{U}$ , and  $\mathbf{Q}_{\mathcal{U}}^{(m)}$  is a matrix formed by keeping in  $\mathbf{Q}^{(m)}$  only the rows and columns corresponding to the ports in set  $\mathcal{U}$ .

In Ref. [22], Eq.(33) is obtained by considering only the Gaussian state of ideal GBS. Furthermore, how to include the effects of partial distinguishability is not obvious from their formalism. Therefore, we need a new expression for  $P(\mathbf{s})$  to include the effects of all  $M+1$  modes and make Eq.(33) a special case. We propose the probability as a weighted sum of the marginal probabilities of no-click events:

$$P(\mathbf{s}) = \sum_{\mathcal{V} \in \mathcal{P}(\mathcal{U})} (-1)^{|\mathcal{U}| - |\mathcal{V}|} \tilde{P}(\mathcal{R}), \quad (35)$$

where  $\tilde{P}(\mathcal{R})$  is the marginal probability of a no-click event for the ports in the given set  $\mathcal{R}$  with the expression:

$$\tilde{P}(\mathcal{R}) = \prod_{m'=0}^M \tilde{P}^{(m')}(\mathcal{R}). \quad (36)$$

Here,  $\mathcal{R}$  is the set difference of  $[1, M]$  and  $\mathcal{V}$  i.e.  $\mathcal{R} = [1, M] - \mathcal{V}$ .  $\tilde{P}^{(m')}(\mathcal{R})$  is the marginal probability of a no-click event in the  $m'$ th mode.

For Gaussian states the marginal probability distribution of certain ports can be directly calculated by only considering the columns and rows corresponding to

these ports in the covariance matrix. Additionally, the marginal probability of a no-click event is a function of determinant, therefore we have

$$\tilde{P}^{(m')}(\mathcal{R}) = \frac{1}{\sqrt{\det(\mathbf{Q}_{\mathcal{R}}^{(m')})}}. \quad (37)$$

When  $\eta_{\text{ind}} = 1$ , all photons are indistinguishable hence there is no click in any  $m$ th virtual mode such that  $\tilde{P}^{(m)}(\mathcal{R}) = 1$ . By proving that

$$\det(\mathbf{Q}_{\mathcal{R}}^{(0)}) = \det(\mathbf{Q}^{(0)}) \det\left(\left(\mathbf{Q}^{(0)-1}\right)_{\mathcal{V}}\right), \quad (38)$$

Eq.(33) becomes a special case of Eq.(35). The proof is given in Appendix C. Apparently,  $\det(\mathbf{Q}^{(0)})$  is irreducible so that the complexity of calculating  $\tilde{P}^{(0)}(\mathcal{R})$  remains  $O(|\mathcal{R}|^3)$  as in the case of Torontonian.

Interestingly, the marginal probability of a no-click events in all virtual modes can be reduced to

$$\tilde{P}^{(m)}(\mathcal{R}) = \frac{1}{\sqrt{(1 + \mathcal{T}_m(\mathcal{R})\alpha_d)^2 - (\mathcal{T}_m(\mathcal{R})\beta_d)^2}}, \quad (39)$$

where  $\mathcal{T}_m(\mathcal{R}) = \sum_{j \in \mathcal{R}} |T_{j,m}|^2$ . A detailed derivation of Eq.(39) can be found in Appendix D.  $\mathcal{T}_m(\mathcal{R})$  can be interpreted as the total transmission rate of ports in  $\mathcal{R}$ . When  $\eta_{\text{ind}} = 1$ ,  $\alpha_d = \beta_d = 0$  we have  $\tilde{P}^{(m)}(\mathcal{R}) = 1$ . This gives an exact calculation of the probability distribution of threshold detector GBS with partial distinguishability.

## VI. QUANTUM SUPREMACY WITH PARTIALLY DISTINGUISHABLE GAUSSIAN BOSON SAMPLING

We have obtained the probability distribution of partially distinguishable GBS that does not require any assumptions of being collision-free, or having a determinate photon number and explicitly include losses. We proceed to discuss how partial distinguishability affects quantum supremacy.

Let us define an approximate version of the probability  $P(\mathbf{s})$  by replacing  $P_{\text{dis}}(\mathbf{s})$  with  $P_{\text{sim}}(\mathbf{s}, \varepsilon)$  and truncating Eq.(19) at a certain value  $N_{\text{cut}}$

$$P_{\text{approx}}(\mathbf{s}, \varepsilon, N_{\text{cut}}) = \sum_{n=0}^{N_{\text{cut}}} P_n(\mathbf{s}, \varepsilon), \quad (40)$$

$$P_n(\mathbf{s}, \varepsilon) = \sum_{\mathbf{s}_n^{(0)}} P^{(0)}(\mathbf{s}_n^{(0)}) P_{\text{sim}}(\mathbf{s} - \mathbf{s}_n^{(0)}, \varepsilon). \quad (41)$$

Here,  $P_n(\mathbf{s}, \varepsilon)$  includes the contributions of all configurations that have  $n$  indistinguishable photons. The magnitude of this term depends on the indistinguishability efficiency  $\eta_{\text{ind}}$ . For the extreme condition that  $\eta_{\text{ind}} = 1$  which corresponds to the ideal case,  $P_n(\mathbf{s}, \varepsilon)$  from  $n < N$  are all zero. Since the dependence of  $P_n(\mathbf{s}, \varepsilon)$  on  $n$  for

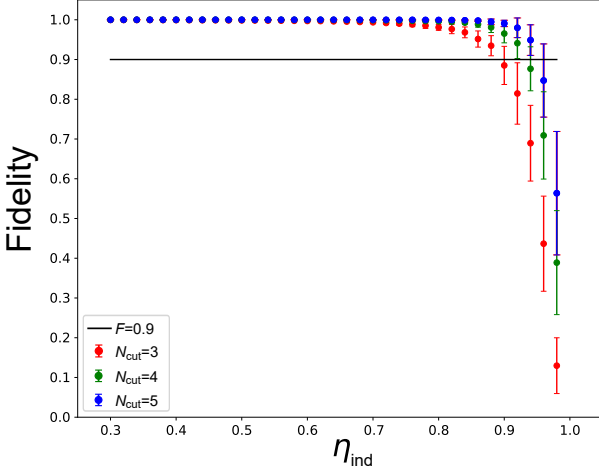


FIG. 2. Numerical evaluations of fidelity for  $N_{\text{cut}} = 3, N_{\text{cut}} = 4$  and  $N_{\text{cut}} = 5$  when  $K = 35, M = 6, N = 6, r = 0.9, \eta_t = 0.9$ . The output pattern is  $s_1 = \dots = s_N = 1, s_{N+1} = \dots = s_K = 0$  the other choices of output pattern give similar results. This result is obtained over 94 Haar-random unitary matrices.

$\eta_{\text{ind}} < 1$  is approximately exponentially decreasing, we may safely truncate  $P_{\text{approx}}$  with  $N_{\text{cut}}$  smaller than  $N$ . Such an approximation can achieve high fidelity, which we define as

$$F(\mathbf{s}, \varepsilon, N_{\text{cut}}) = P_{\text{approx}}(\mathbf{s}, \varepsilon, N_{\text{cut}}) / P(\mathbf{s}). \quad (42)$$

This approximation is powerful because the computational complexity increases superexponentially with  $N_{\text{cut}}$ . This is because the computational complexity of calculating  $P^{(0)}(\mathbf{s}_n^{(0)})$  is  $O(n^3 2^n)$  which is exponential and the number of elements in  $\mathbf{s}_n^{(0)}$  is polynomial respect to  $n$ . The complexity of  $P_{\text{approx}}(\mathbf{s}, \varepsilon, N_{\text{cut}})$  with regard to  $N_{\text{cut}}$  is  $O(\text{poly}(N_{\text{cut}}) 2^{N_{\text{cut}}})$ . Considering that ideal GBS has a complexity  $O(N^3 2^N)$ , for sufficiently large  $N$ , every term dropped in Eq.(40) gives a large saving in comparison to calculating the ideal GBS.

We have not been able to obtain an analytical relationship between  $F$  and  $\eta_{\text{ind}}$ . However, numerically we observe that the fidelity obeys an approximate relation

$$F \approx 1 - ce^{\eta_{\text{ind}}}, \quad (43)$$

as shown in Fig.2, where  $c$  is a fitting parameter. According to this relation, the approximation can achieve high fidelity for  $N_{\text{cut}}$  much smaller than  $N$  unless  $\eta_{\text{ind}}$  is close to 1. In Fig.2 we show the approximation for various  $N_{\text{cut}}$ . We see that the fidelity is above 0.9 even for a modest  $N_{\text{cut}} = 3$  approximation with  $\eta_{\text{ind}}$  as large as 0.9. We note that this is  $2^{N-3}$  times faster than a calculation of ideal GBS.

Another observation is that for a given GBS set up, when the total number of photons of an output pattern

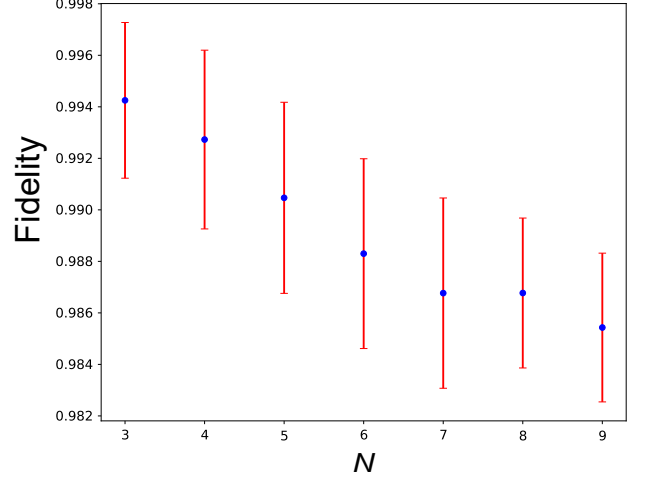


FIG. 3. Numerical evaluations of fidelity for  $P_{\text{approx}}(N_{\text{cut}} = 2)$  with increasing number of detected photons  $N$  when  $K = 30, M = 6, r = 0.9, \eta_{\text{ind}} = 0.5, \eta_t = 0.9$ . The output pattern for each  $N$  is  $s_1 = \dots = s_N = 1, s_{N+1} = \dots = s_K = 0$ , the other choices of output pattern give similar results. This result is obtained over 94 Haar-random unitary matrices.

increases while the order of an approximation  $N_{\text{cut}}$  is fixed, the fidelity of the  $P_{\text{approx}}$  only decreases linearly or even more slowly. For the example shown in Fig.3, we use  $P_{\text{approx}}(N_{\text{cut}} = 2)$  to approximate the output patterns for a total number of photons  $N$ , from 3 to 9. While the exact calculation of these output patterns requires an exponential increase in computational time, the fidelity of the approximation  $P_{\text{approx}}(N_{\text{cut}} = 2)$  does not decrease exponentially. Instead, it decreases linearly. At a particular  $N$ , the rate of decrease eases. Such trade-off between fidelity and computational time shows the effectiveness of this approximation method.

For GBS with threshold detectors, partial distinguishability does not affect quantum supremacy directly because the main exponential contribution to the complexity comes from the number of elements to be calculated, which is  $2^N$ . Partial distinguishability only reduces the complexity of calculating one element from  $O(N^3)$  to  $O(N)$ , by converting calculation of the determinant to multiplication as shown in Eq.(39). We note that if we let  $\eta_{\text{ind}} \approx 0$  such that all photons are almost distinguishable, the computational complexity is still exponential because the number of elements is still  $2^N$  which is established as the proof for exponential complexity for GBS with threshold detectors. But clearly the sampling method for  $P_{\text{sim}}(\mathbf{s}, \varepsilon)$  can be used in this case as well.

## VII. CONCLUSION

In this paper we have developed a model which allows us to model GBS with partially distinguishable pho-

tons and obtain the expressions for the probabilities of a given output pattern for both PNR and threshold detectors. The model is based on the construction of virtual modes which incorporates the distinguishable photons and forms a new Gaussian state that propagates inside the interferometer independently until it reaches the detectors. We have proved that the expression for the probability of the photons from these distinguishable Gaussian states contains the previous result obtained by Aaronson and Arkhipov for the distinguishable AABS as a special case. This is because we included the indeterminate-photon-number nature of Gaussian states in contrast to AABS where the photon number is fixed. Based on that we proposed an algorithm for efficient simulation of the output patterns from these distinguishable Gaussian states which enables us to exponentially reduce the computational time of calculating the probabilities.

Our method provides a framework to calculate the probabilities for imperfect GBS, especially for GBS with threshold detectors which has only been theoretically investigated for the ideal case. We proved that the Torontonian — the result obtained in the ideal case — is a special case within our framework. We note that for low indistinguishability efficiency, the proof that supports the complexity of computing the Torontonian still holds. Our aforementioned simulation algorithm can reduce the computationally hard exact calculation with a highly accurate approximation particularly for low indistinguishability.

For GBS with PNR detectors, which to date is more theoretically developed, we proposed an approximation based on the structure of the expression of the probability with respect to indistinguishability efficiency to show how partial distinguishability affects quantum supremacy. We take advantage of the physical nature of the indistinguishability, i.e. interference of photons which is the cause of the computationally-hard complexity. Therefore for low indistinguishability, we only include contributions from a smaller number of interfering photons which takes exponentially less time. According to our simulations, such an approximation can achieve above 90% fidelity even in the case of indistinguishability efficiency up to  $\eta_{\text{ind}} = 0.9$ . Numerically we showed how the computational time of our approximation for a given fidelity decreases exponentially with the decrease of indistinguishable efficiency which indicates the relationship between partial distinguishability and quantum supremacy.

We note that although we have obtained the expression Eq.(35) for the exact calculation of the probability for GBS with threshold detectors, using that expression to find an approximation method is less easily constructed, unlike the case for PNR detectors. For the PNR detector case, the approximation Eq.(40) comes naturally from the expression Eq.(17) for exact sampling. In this sense, GBS with threshold detectors is advantageous than GBS with PNR detectors in the context of quantum supremacy due to the lack of an efficient approximation algorithm. For PNR detectors, our approximation

method delineates the bound of indistinguishability efficiency for efficient simulation at a required fidelity and computational time. Generally speaking, the indistinguishability efficiency should be larger than 0.9, which is satisfied for the recent GBS experiments to date [19–21]. In this sense, we find that the claims of Ref. [21] to be in the quantum supremacy regime consistent with our analysis. We do not, however, rule out the possibility that an analogous classically efficient algorithm for threshold detectors could be developed. The question in this case would be what level of indistinguishability efficiency would be required such that quantum supremacy would be attainable.

## ACKNOWLEDGMENTS

This work is supported by the National Natural Science Foundation of China (62071301); State Council of the People’s Republic of China (D1210036A); NSFC Research Fund for International Young Scientists (11850410426); NYU-ECNU Institute of Physics at NYU Shanghai; the Science and Technology Commission of Shanghai Municipality (19XD1423000); the China Science and Technology Exchange Center (NGA-16-001).

## Appendix A: Q-function covariance matrices and kernel matrices of all $M+1$ modes

As shown in Eq.(16), the probability of obtaining a certain output pattern  $\mathbf{s}$  from a Gaussian state requires the covariance matrix of the Q-function of the state, denoted as  $\mathbf{Q}$ . It is needed for the value of its determinant and for constructing the kernel matrix  $\mathbf{A}$ :

$$\mathbf{A} = \begin{bmatrix} \mathbf{0} & \mathbf{I}_K \\ \mathbf{I}_K & \mathbf{0} \end{bmatrix} (\mathbf{I}_{2K} - \mathbf{Q}^{-1}). \quad (\text{A1})$$

$\mathbf{Q}$  is converted from the real covariance matrix  $\mathbf{V}$  and hence from Eq.(8) and Eq.(9) we obtain  $\mathbf{Q}$  for all  $M+1$  modes :

$$\mathbf{Q}^{(0)} = \mathbf{I}_{2K} + \begin{bmatrix} \mathbf{T} & \mathbf{0} \\ \mathbf{0} & \mathbf{T}^* \end{bmatrix} \begin{bmatrix} \mathbf{D}_\alpha & \mathbf{D}_\beta \\ \mathbf{D}_\beta & \mathbf{D}_\alpha \end{bmatrix} \begin{bmatrix} \mathbf{T}^\dagger & \mathbf{0} \\ \mathbf{0} & \mathbf{T}^T \end{bmatrix}, \quad (\text{A2})$$

$$\mathbf{Q}^{(m)} = \mathbf{I}_{2K} + \begin{bmatrix} \alpha_d \mathbf{E}_{2,m} & \beta_d \mathbf{E}_{1,m} \\ \beta_d \mathbf{E}_{1,m}^* & \alpha_d \mathbf{E}_{2,m}^* \end{bmatrix}, \quad (\text{A3})$$

where the contained matrices and coefficients are given by

$$\mathbf{D}_\alpha = \bigoplus_{j=1}^M \alpha_i \bigoplus_{j=1}^{K-M} 0, \quad (A4)$$

$$\mathbf{D}_\beta = \bigoplus_{j=1}^M \beta_i \bigoplus_{j=1}^{K-M} 0, \quad (A5)$$

$$\mathbf{E}_{1,m} = \begin{bmatrix} T_{1,m} \\ \vdots \\ T_{K,m} \end{bmatrix} [T_{1,m} \ \cdots \ T_{K,m}], \quad (A6)$$

$$\mathbf{E}_{2,m} = \begin{bmatrix} T_{1,m} \\ \vdots \\ T_{K,m} \end{bmatrix} [T_{1,m}^* \ \cdots \ T_{K,m}^*], \quad (A7)$$

$$\alpha_i = \eta_t \eta_{\text{ind}} \sinh r \sinh r, \quad (A8)$$

$$\beta_i = \eta_t \eta_{\text{ind}} \sinh r \cosh r, \quad (A9)$$

$$\alpha_d = \eta_t (1 - \eta_{\text{ind}}) \sinh r \sinh r, \quad (A10)$$

$$\beta_d = \eta_t (1 - \eta_{\text{ind}}) \sinh r \cosh r. \quad (A11)$$

It is easy to see that  $\alpha_i$  is the average number of photons from the indistinguishable mode and  $\alpha_d$  is the average number of photons from  $m$ th virtual mode.

Directly calculating  $\mathbf{Q}^{-1}$  is very difficult, so instead we obtain the kernel matrix in two steps: first, we pick out the effect of the transformation matrix that we are allowed to calculate the kernel matrix of the input:

$$\mathbf{A} = \begin{bmatrix} \mathbf{T}^* & \mathbf{0} \\ \mathbf{0} & \mathbf{T} \end{bmatrix} \begin{bmatrix} \mathbf{0} & \mathbf{I}_K \\ \mathbf{I}_K & \mathbf{0} \end{bmatrix} (\mathbf{I}_{2K} - \mathbf{Q}^{-1}) \begin{bmatrix} \mathbf{T}^\dagger & \mathbf{0} \\ \mathbf{0} & \mathbf{T}^T \end{bmatrix}. \quad (A12)$$

Second, we notice that the structure of  $\mathbf{Q}$  is the sum of the identity matrix and a matrix constructed from four diagonal submatrices. We take advantage of this structure to bypass  $\mathbf{Q}^{-1}$  and obtain the expression of  $\mathbf{I}_{2K} - \mathbf{Q}^{-1}$ :

$$\begin{aligned} & \left( \mathbf{I}_{2K} + \begin{bmatrix} \alpha \mathbf{I}_K & \beta \mathbf{I}_K \\ \beta \mathbf{I}_K & \alpha \mathbf{I}_K \end{bmatrix} \right) \left( \mathbf{I}_{2K} - \begin{bmatrix} \alpha' \mathbf{I}_K & \beta' \mathbf{I}_K \\ \beta' \mathbf{I}_K & \alpha' \mathbf{I}_K \end{bmatrix} \right) = \mathbf{I}_{2K}, \\ & \Rightarrow \begin{cases} \alpha' = 1 - \frac{1 + \alpha}{(1 + \alpha)^2 - \beta^2}, \\ \beta' = \frac{\beta}{(1 + \alpha)^2 - \beta^2}. \end{cases} \end{aligned}$$

The physical meanings of these two coefficients are shown in the following:

$$\alpha' = \frac{\langle (\Delta \hat{q})^2 \rangle \langle (\Delta \hat{p})^2 \rangle - 1}{(1 + \langle (\Delta \hat{q})^2 \rangle)(1 + \langle (\Delta \hat{p})^2 \rangle)}, \quad (A13)$$

$$\beta' = \frac{1}{4} \frac{\langle (\Delta \hat{q})^2 \rangle - \langle (\Delta \hat{p})^2 \rangle}{(1 + \langle (\Delta \hat{q})^2 \rangle)(1 + \langle (\Delta \hat{p})^2 \rangle)}. \quad (A14)$$

In this way we are able to obtain the kernel matrix for the indistinguishable mode:

$$\mathbf{A}^{(0)} = \begin{bmatrix} \mathbf{T}^* & \mathbf{0} \\ \mathbf{0} & \mathbf{T} \end{bmatrix} \begin{bmatrix} \mathbf{D}'_\beta & \mathbf{D}'_\alpha \\ \mathbf{D}'_\alpha & \mathbf{D}'_\beta \end{bmatrix} \begin{bmatrix} \mathbf{T}^\dagger & \mathbf{0} \\ \mathbf{0} & \mathbf{T}^T \end{bmatrix}, \quad (A15)$$

where

$$\mathbf{D}'_\alpha = \bigoplus_{j=1}^M \alpha'_i \bigoplus_{j=1}^{K-M} 0, \quad (A16)$$

$$\mathbf{D}'_\beta = \bigoplus_{j=1}^M \beta'_i \bigoplus_{j=1}^{K-M} 0, \quad (A17)$$

$$\alpha'_i = \frac{(1 - \eta_{\text{ind}} \eta_t) \eta_{\text{ind}} \eta_t \sinh^2 r}{1 + \eta_t \eta_{\text{ind}} (2 - \eta_t \eta_{\text{ind}}) \sinh^2 r}, \quad (A18)$$

$$\beta'_i = \frac{\eta_t \eta_{\text{ind}} \sinh r \cosh r}{1 + \eta_t \eta_{\text{ind}} (2 - \eta_t \eta_{\text{ind}}) \sinh^2 r}. \quad (A19)$$

For the virtual modes, their kernel matrices bear a different form:

$$\mathbf{A}^{(m)} = \begin{bmatrix} \beta'_d \mathbf{E}_{1,m}^* & \alpha'_d \mathbf{E}_{2,m}^* \\ \alpha'_d \mathbf{E}_{2,m} & \beta'_d \mathbf{E}_{1,m} \end{bmatrix}, \quad (A20)$$

where expressions for  $\alpha'_d$  and  $\beta'_d$  can be found in Eq.(26) and Eq.(27).

## Appendix B: Derivation of Eq.(23)

To obtain Eq.(23), firstly we need to calculate  $\text{Haf}(\mathbf{A}^{(m)})$  where the form of  $\mathbf{A}^{(m)}$  is given by Eq.(A20). Direct calculation is very difficult so we observe that  $\mathbf{A}^{(m)}$  can be decomposed into two matrices with no overlap:

$$\mathbf{A}^{(m)} = \beta'_d \begin{bmatrix} \mathbf{E}_{1,m}^* & 0 \\ 0 & \mathbf{E}_{1,m} \end{bmatrix} + \alpha'_d \begin{bmatrix} 0 & \mathbf{E}_{2,m}^* \\ \mathbf{E}_{2,m} & 0 \end{bmatrix}. \quad (B1)$$

Combined with the definition of Hafnian function we obtain

$$\text{Haf}(\mathbf{A}^{(m)}) = \frac{1}{n! 2^n} \sum_{\rho \in S_{2n}} \prod_{j=1}^n G_{\rho(2j-1), \rho(2j)} H_{\rho(2j-1), \rho(2j)}, \quad (B2)$$

where we have

$$\mathbf{G} = \begin{bmatrix} \mathbf{E}_{1,m}^* & \mathbf{E}_{2,m}^* \\ \mathbf{E}_{2,m} & \mathbf{E}_{1,m} \end{bmatrix} \quad (B3)$$

and  $\mathbf{H}$  is a  $2n \times 2n$  matrix such that

$$H_{i,j} = \begin{cases} \beta'_d, & \text{if } (i > n \text{ AND } j > n) \text{ OR } (i \leq n \text{ AND } j \leq n) \\ \alpha'_d, & \text{if } (i > n \text{ AND } j \leq n) \text{ OR } (i \leq n \text{ AND } j > n). \end{cases} \quad (B4)$$

With the definitions Eq.(A6) and Eq.(A7), it is easy to prove that

$$\prod_{j=1}^n G_{\rho(2j-1), \rho(2j)} = \prod_{i=1}^K |T_{k,m}|^{2s_k^{(m)}}, \quad (B5)$$

which can be used to reduce the calculation of  $\text{Haf}(\mathbf{A}^{(m)})$  to the calculation of  $\text{Haf}(\mathbf{H})$ :

$$\text{Haf}(\mathbf{A}^{(m)}) = \prod_{k=1}^K |T_{k,m}|^{2s_k^{(m)}} \text{Haf}(\mathbf{H}). \quad (B6)$$

The calculation of  $\text{Haf}(\mathbf{H})$  is non-trivial and we must resort to graph theory. As is well-known, the Hafnian is closely linked to weighted perfect matchings of a graph by the following definition for a  $2n \times 2n$  matrix:

$$\text{Haf}(\mathbf{H}) = \sum_{\tau \in \text{PMP}(2n)} \prod_{(i,j) \in \tau} H_{i,j}, \quad (\text{B7})$$

which means we have to perfectly match  $2n$  vertices to form one permutation in  $\text{PMP}(2n)$ .

Regarding the definition of  $H_{i,j}$ , we can divide these  $2n$  vertices into two sets:  $\mathcal{N}_1 = [1, n]$  and  $\mathcal{N}_2 = [n+1, 2n]$ . A match inside  $\mathcal{N}_1$  or  $\mathcal{N}_2$  corresponds to the weight  $\beta'_d$  and the match between  $\mathcal{N}_1$  and  $\mathcal{N}_2$  corresponds to the weight  $\alpha'_d$ . For a given permutation, if we denote the number of matches inside  $\mathcal{N}_1$  or  $\mathcal{N}_2$  as  $q$ , the number of matches between  $\mathcal{N}_1$  and  $\mathcal{N}_2$  is consequently  $n - q$ . Note the value of  $q$  is always even because a match in  $\mathcal{N}_1$  inevitably leads to a match in  $\mathcal{N}_2$ . Now we can rewrite  $\text{Haf}(\mathbf{H})$  as a summation respect to  $q$ :

$$\text{Haf}(\mathbf{H}) = \sum_q f_q \beta'_d^q \alpha'_d^{n-q}, \quad (\text{B8})$$

where  $q \in \{0, 2, \dots, 2\lfloor \frac{n}{2} \rfloor\}$ .

The final step is to obtain the expression of  $f_q$ . Firstly, we regroup the vertices in  $\mathcal{N}_1$  into two sets:  $\mathcal{N}_{1,\text{in}}$  contains the vertices matching vertices inside  $\mathcal{N}_1$ ;  $\mathcal{N}_{1,\text{out}}$  contains the vertices matching vertices in  $\mathcal{N}_2$ . We do the same thing for vertices in  $\mathcal{N}_2$  such that in total there are  $\left(\frac{n!}{q!(n-q)!}\right)^2$  configurations for this process.

Secondly, we count the number of perfect matches for vertices in  $\mathcal{N}_{1,\text{in}}$  and  $\mathcal{N}_{2,\text{in}}$ . Since each one contributes  $|\text{PMP}(q)| = (q-1)!!$  permutations, in total there are  $((q-1)!!)^2$  configurations in this process.

Thirdly, we count the number of matches between vertices in  $\mathcal{N}_{1,\text{out}}$  and  $\mathcal{N}_{2,\text{out}}$ . Since there are  $n-q$  vertices in each set, we can straightforwardly obtain the number of configurations to be  $(n-q)!$ .

Combining them we obtain the closed-form expression of  $f_p$ :

$$\begin{aligned} f_p &= \left(\frac{n!}{q!(n-q)!}\right)^2 ((q-1)!!)^2 (n-q)! \\ &= \frac{(n!)^2}{(q!!)^2 (n-q)!}. \end{aligned} \quad (\text{B9})$$

It is easy to prove that  $\sum_q f_q = (2n-1)!!$ , which verifies the correctness of the expression.

Thus we obtain the analytical result for  $\text{Haf}(\mathbf{A}^{(m)})$  and hence Eq.(23) where we let  $G(N) = \text{Haf}(\mathbf{H})$ .

### Appendix C: Proof of Eq.(38)

This section proves that for a covariance matrix  $\Sigma$  of size  $2K \times 2K$ ,  $\mathcal{U} = [1, K]$ ,  $\mathcal{R}$  is an arbitrary subset of  $\mathcal{U}$ ,

$\mathcal{R}^c$  is the relative complement set of  $\mathcal{R}$  respect to  $\mathcal{U}$ , we will always have:

$$\det(\Sigma_{\mathcal{R}}) = \det(\Sigma) \det\left((\Sigma^{(-1)})_{\mathcal{R}^c}\right). \quad (\text{C1})$$

*Proof:* First, we regroup the matrix  $\Sigma$  as  $\begin{bmatrix} \mathbf{A} & \mathbf{B} \\ \mathbf{C} & \mathbf{D} \end{bmatrix}$  by moving rows and columns so that  $\mathbf{A}$  includes the indices from  $\mathcal{R}^c$  and  $\mathbf{B}$  includes the indices from  $\mathcal{R}$ . Note the sign of the determinant will not be changed because the interchange of rows (columns) are always carried out an even number of times therefore we have

$$\det(\Sigma) = \det\left(\begin{bmatrix} \mathbf{A} & \mathbf{B} \\ \mathbf{C} & \mathbf{D} \end{bmatrix}\right). \quad (\text{C2})$$

Next, we use the Schur complement

$$\det\left(\begin{bmatrix} \mathbf{A} & \mathbf{B} \\ \mathbf{C} & \mathbf{D} \end{bmatrix}\right) = \det(\mathbf{A} - \mathbf{C}\mathbf{D}^{-1}\mathbf{B}) \det(\mathbf{D}), \quad (\text{C3})$$

to obtain

$$\det(\mathbf{A} - \mathbf{C}\mathbf{D}^{-1}\mathbf{B}) = \frac{\det(\Sigma)}{\det(\Sigma_{\mathcal{R}})}. \quad (\text{C4})$$

Then we calculate the inverse matrix of  $\begin{bmatrix} \mathbf{A} & \mathbf{B} \\ \mathbf{C} & \mathbf{D} \end{bmatrix}$  to be  $\begin{bmatrix} \mathbf{A} - \mathbf{B}\mathbf{D}^{-1}\mathbf{C} & -\mathbf{D}^{-1}\mathbf{C}(\mathbf{A} - \mathbf{B}\mathbf{D}^{-1}\mathbf{C})^{-1} \\ -\mathbf{A}^{-1}\mathbf{B}(\mathbf{D} - \mathbf{C}\mathbf{A}^{-1}\mathbf{B})^{-1} & \mathbf{D} - \mathbf{C}\mathbf{A}^{-1}\mathbf{B} \end{bmatrix}$ . Therefore

$$(\mathbf{A} - \mathbf{C}\mathbf{D}^{-1}\mathbf{B})^{-1} = (\Sigma^{-1})_{\mathcal{R}^c}, \quad (\text{C5})$$

such that we obtain another equation of  $\det(\mathbf{A} - \mathbf{C}\mathbf{D}^{-1}\mathbf{B})$

$$\det(\mathbf{A} - \mathbf{C}\mathbf{D}^{-1}\mathbf{B}) = \frac{1}{\det((\Sigma^{-1})_{\mathcal{R}^c})}. \quad (\text{C6})$$

Combining Eq.(C4) and Eq.(C6) we obtain Eq.(C1).

### Appendix D: Calculation of marginal probability of distinguishable photons

This section calculates the marginal probability of given ports according to Eq.(37). Basically, that amounts to calculating the determinant of a selected covariance matrix  $\mathbf{Q}_{\mathcal{R}}^{(m)}$  whose rows and columns are selected from  $\mathbf{Q}^{(m)}$  according to the ports listed in set  $\mathcal{R}$ . Without loss of generality, we presume there are  $n$  elements in  $\mathcal{R}$  and we denote its  $i$ th element as  $R_i$ .

According to the form of  $\mathbf{Q}^{(m)}$  in Eq.(A3),  $\mathbf{Q}_{\mathcal{R}}^{(m)}$  can be written as a single matrix:

$$\mathbf{Q}_{\mathcal{R}}^{(m)} = \begin{bmatrix} (\gamma_1 + \alpha_d)T_{R_1,m}T_{R_1,m}^* & \dots & \alpha_d T_{R_1,m}T_{R_n,m}^* & \beta_d T_{R_1,m}T_{R_1,m} & \dots & \beta_d T_{R_1,m}T_{R_n,m} \\ \vdots & \ddots & \vdots & \vdots & \ddots & \vdots \\ \alpha_d T_{R_n,m}T_{R_1,m}^* & \dots & (\gamma_n + \alpha_d)T_{R_n,m}T_{R_n,m}^* & \beta_d T_{R_n,m}T_{R_1,m} & \dots & \beta_d T_{R_n,m}T_{R_n,m} \\ \beta_d T_{R_1,m}^*T_{R_1,m} & \dots & \beta_d T_{R_1,m}^*T_{R_n,m} & (\gamma_1 + \alpha_d)T_{R_1,m}^*T_{R_1,m} & \dots & \alpha_d T_{R_1,m}^*T_{R_n,m} \\ \vdots & \ddots & \vdots & \vdots & \ddots & \vdots \\ \beta_d T_{R_n,m}^*T_{R_1,m} & \dots & \beta_d T_{R_n,m}^*T_{R_n,m} & \alpha_d T_{R_n,m}^*T_{R_1,m} & \dots & (\gamma_K + \alpha_d)T_{R_n,m}^*T_{R_n,m} \end{bmatrix} \quad (D1)$$

where  $\gamma_i = 1/|T_{R_i,m}|^2$ . Now we take all the coefficients and form another matrix  $\mathbf{C}$ :

$$\mathbf{C} = \begin{bmatrix} \gamma_1 + \alpha_d & \dots & \alpha_d & \beta_d & \dots & \beta_d \\ \vdots & \ddots & \vdots & \vdots & \ddots & \vdots \\ \alpha_d & \dots & \gamma_K + \alpha_d & \beta_d & \dots & \beta_d \\ \beta_d & \dots & \beta_d & \gamma_1 + \alpha_d & \dots & \alpha_d \\ \vdots & \ddots & \vdots & \vdots & \ddots & \vdots \\ \beta_d & \dots & \beta_d & \alpha_d & \dots & \gamma_K + \alpha_d \end{bmatrix}. \quad (D2)$$

Then we calculate its determinant by resorting to the definition of determinant

$$\begin{aligned} \det(\mathbf{Q}_{\mathcal{R}}^{(m)}) &= \sum_{\rho \in S_{2K}} \text{Sgn}(\rho) \prod_{i=1}^{2n} \mathbf{Q}_{\mathcal{R}}^{(m)}(i, \rho(i)) \\ &= \sum_{\rho \in S_{2K}} \text{Sgn}(\rho) \prod_{i=1}^{2n} \mathbf{C}_{i, \rho(i)} \left( \prod_{j=1}^n |T_{R_j,m}|^2 \right)^2 \\ &= \frac{1}{\mathcal{C}^2} \det(\mathbf{C}), \end{aligned} \quad (D3)$$

where  $\mathcal{C} = \sum_{j=1}^n 1/\gamma_j$ . Consequently we have

$$\det(\mathbf{Q}_{\mathcal{R}}^{(m)}) = (1 + \mathcal{T}\alpha_d)^2 - (\mathcal{T}\beta_d)^2. \quad (D5)$$

where  $\mathcal{C} = \prod_{j=1}^n \gamma_j^2$ . Then we find that

$$\det(\mathbf{C}) = (\mathcal{C} + \mathcal{C}\mathcal{T}(\alpha_d - \beta_d))(\mathcal{C} + \mathcal{C}\mathcal{T}(\alpha_d + \beta_d)), \quad (D4)$$

We then use this in Eq.(37) to obtain Eq.(39).

---

[1] S. Aaronson and A. Arkhipov, The Computational Complexity of Linear Optics, *Theory of Computing* **9**, 143 (2013).

[2] F. Arute, K. Arya, R. Babbush, D. Bacon, J. C. Bardin, R. Barends, R. Biswas, S. Boixo, F. G. S. L. Brandao, D. A. Buell, B. Burkett, Y. Chen, Z. Chen, B. Chiaro, R. Collins, W. Courtney, A. Dunsworth, E. Farhi, B. Foxen, A. Fowler, C. Gidney, M. Giustina, R. Graff, K. Guerin, S. Habegger, M. P. Harrigan, M. J. Hartmann, A. Ho, M. Hoffmann, T. Huang, T. S. Humble, S. V. Isakov, E. Jeffrey, Z. Jiang, D. Kafri, K. Kechedzhi, J. Kelly, P. V. Klimov, S. Knysh, A. Korotkov, F. Kostritsa, D. Landhuis, M. Lindmark, E. Lucero, D. Lyakh, S. Mandrà, J. R. McClean, M. McEwen, A. Megrant, X. Mi, K. Michielsen, M. Mohseni, J. Mutus, O. Naaman, M. Neeley, C. Neill, M. Y. Niu, E. Ostby, A. Petukhov, J. C. Platt, C. Quintana, E. G. Rieffel, P. Roushan, N. C. Rubin, D. Sank, K. J. Satzinger, V. Smelyanskiy, K. J. Sung, M. D. Trevithick, A. Vainsencher, B. Villalonga, T. White, Z. J. Yao, P. Yeh, A. Zalcman, H. Neven, and J. M. Martinis, Quantum supremacy using a programmable superconducting processor, *Nature* **574**, 505 (2019).

[3] E. Pednault, J. A. Gunnels, G. Nannicini, L. Horesh, and R. Wisnieff, Leveraging Secondary Storage to Simulate Deep 54-qubit Sycamore Circuits, arXiv:1910.09534 (2019).

[4] F. Pan and P. Zhang, Simulating the Sycamore quantum supremacy circuits, arXiv:2103.03074 (2021).

[5] L. Valiant, The complexity of computing the permanent, *Theoretical Computer Science* **8**, 189 (1979).

[6] S. Scheel, Permanents in linear optical networks, arXiv:quant-ph/0406127 (2004).

[7] A. Neville, C. Sparrow, R. Clifford, E. Johnston, P. M.

Birchall, A. Montanaro, and A. Laing, Classical boson sampling algorithms with superior performance to near-term experiments, *Nature Physics* **13**, 1153 (2017).

[8] H. Wang, Y. He, Y.-H. Li, Z.-E. Su, B. Li, H.-L. Huang, X. Ding, M.-C. Chen, C. Liu, J. Qin, J.-P. Li, Y.-M. He, C. Schneider, M. Kamp, C.-Z. Peng, S. Höfling, C.-Y. Lu, and J.-W. Pan, High-efficiency multiphoton boson sampling, *Nature Photonics* **11**, 361 (2017).

[9] Y. He, X. Ding, Z.-E. Su, H.-L. Huang, J. Qin, C. Wang, S. Unsleber, C. Chen, H. Wang, Y.-M. He, X.-L. Wang, W.-J. Zhang, S.-J. Chen, C. Schneider, M. Kamp, L.-X. You, Z. Wang, S. Höfling, C.-Y. Lu, and J.-W. Pan, Time-Bin-Encoded Boson Sampling with a Single-Photon Device, *Physical Review Letters* **118**, 190501 (2017).

[10] J. Loredo, M. Broome, P. Hilaire, O. Gazzano, I. Sagnes, A. Lemaitre, M. Almeida, P. Senellart, and A. White, Boson Sampling with Single-Photon Fock States from a Bright Solid-State Source, *Physical Review Letters* **118**, 130503 (2017).

[11] H. Wang, J. Qin, X. Ding, M.-C. Chen, S. Chen, X. You, Y.-M. He, X. Jiang, L. You, Z. Wang, C. Schneider, J. J. Renema, S. Höfling, C.-Y. Lu, and J.-W. Pan, Boson Sampling with 20 Input Photons and a 60-Mode Interferometer in a 10 14-Dimensional Hilbert Space, *Physical Review Letters* **123**, 250503 (2019).

[12] A. Lund, A. Laing, S. Rahimi-Keshari, T. Rudolph, J. O'Brien, and T. Ralph, Boson Sampling from a Gaussian State, *Physical Review Letters* **113**, 100502 (2014).

[13] S. Barkhofen, T. J. Bartley, L. Sansoni, R. Kruse, C. S. Hamilton, I. Jex, and C. Silberhorn, Driven Boson Sampling, *Physical Review Letters* **118**, 020502 (2017).

[14] C. S. Hamilton, R. Kruse, L. Sansoni, S. Barkhofen, C. Silberhorn, and I. Jex, Gaussian Boson Sampling, *Physical Review Letters* **119**, 170501 (2017).

[15] R. Kruse, C. S. Hamilton, L. Sansoni, S. Barkhofen, C. Silberhorn, and I. Jex, Detailed study of Gaussian boson sampling, *Physical Review A* **100**, 032326 (2019).

[16] E. R. Caianiello, *Combinatorics and renormalization in quantum field theory* (W. A. Benjamin, Inc, 1973).

[17] J. M. Arrazola and T. R. Bromley, Using Gaussian Boson Sampling to Find Dense Subgraphs, *Physical Review Letters* **121**, 030503 (2018).

[18] J. Huh, G. G. Guerreschi, B. Peropadre, J. R. McClean, and A. Aspuru-Guzik, Boson sampling for molecular vibronic spectra, *Nature Photonics* **9**, 615 (2015).

[19] H.-S. Zhong, L.-C. Peng, Y. Li, Y. Hu, W. Li, J. Qin, D. Wu, W. Zhang, H. Li, L. Zhang, Z. Wang, L. You, X. Jiang, L. Li, N.-L. Liu, J. P. Dowling, C.-Y. Lu, and J.-W. Pan, Experimental Gaussian Boson sampling, *Science Bulletin* **64**, 511 (2019).

[20] S. Paesani, Y. Ding, R. Santagati, L. Chakhmakhchyan, C. Vigliar, K. Rottwitt, L. K. Oxenløwe, J. Wang, M. G. Thompson, and A. Laing, Generation and sampling of quantum states of light in a silicon chip, *Nature Physics* **15**, 925 (2019).

[21] H.-S. Zhong, H. Wang, Y.-H. Deng, M.-C. Chen, L.-C. Peng, Y.-H. Luo, J. Qin, D. Wu, X. Ding, Y. Hu, P. Hu, X.-Y. Yang, W.-J. Zhang, H. Li, Y. Li, X. Jiang, L. Gan, G. Yang, L. You, Z. Wang, L. Li, N.-L. Liu, C.-Y. Lu, and J.-W. Pan, Quantum computational advantage using photons, *Science (New York, N.Y.)* **370**, 1460 (2020).

[22] N. Quesada, J. M. Arrazola, and N. Killoran, Gaussian boson sampling using threshold detectors, *Physical Review A* **98**, 062322 (2018).

[23] Y. Li, M. Chen, Y. Chen, H. Lu, L. Gan, C. Lu, J. Pan, H. Fu, and G. Yang, Benchmarking 50-Photon Gaussian Boson Sampling on the Sunway TaihuLight, *arXiv:2009.01177* (2020).

[24] S. Rahimi-Keshari, T. C. Ralph, and C. M. Caves, Sufficient Conditions for Efficient Classical Simulation of Quantum Optics, *Physical Review X* **6**, 021039 (2016).

[25] M. Oszmaniec and D. J. Brod, Classical simulation of photonic linear optics with lost particles, *New Journal of Physics* **20**, 092002 (2018).

[26] V. S. Shchesnovich, Noise in boson sampling and the threshold of efficient classical simulability, *Physical Review A* **100**, 012340 (2019).

[27] P. P. Rohde, Optical quantum computing with photons of arbitrarily low fidelity and purity, *Physical Review A* **86**, 052321 (2012).

[28] M. C. Tichy, K. Mayer, A. Buchleitner, and K. Mølmer, Stringent and Efficient Assessment of Boson-Sampling Devices, *Physical Review Letters* **113**, 020502 (2014).

[29] V. S. Shchesnovich, Partial indistinguishability theory for multiphoton experiments in multiport devices, *Physical Review A* **91**, 013844 (2015).

[30] M. C. Tichy, Sampling of partially distinguishable bosons and the relation to the multidimensional permanent, *Physical Review A* **91**, 022316 (2015).

[31] J. Renema, A. Menssen, W. Clements, G. Triginer, W. Kolthammer, and I. Walmsley, Efficient Classical Algorithm for Boson Sampling with Partially Distinguishable Photons, *Physical Review Letters* **120**, 220502 (2018).

[32] H. Qi, D. J. Brod, N. Quesada, and R. García-Patrón, Regimes of Classical Simulability for Noisy Gaussian Boson Sampling, *Physical Review Letters* **124**, 100502 (2020).

[33] J. J. Renema, Simulability of partially distinguishable superposition and Gaussian boson sampling, *Physical Review A* **101**, 063840 (2020).

[34] S. Aaronson and A. Arkhipov, BosonSampling Is Far From Uniform, *Quantum Info. Comput.* **14**, 1383 (2014).

[35] A. Ferraro, S. Olivares, and M. G. A. Paris, Gaussian states in continuous variable quantum information, *arXiv:quant-ph/0503237* (2005).

[36] C. Weedbrook, S. Pirandola, R. García-Patrón, N. J. Cerf, T. C. Ralph, J. H. Shapiro, and S. Lloyd, Gaussian quantum information, *Reviews of Modern Physics* **84**, 621 (2012).

[37] S. Barnett and P. Radmore, *Methods in theoretical quantum optics*, Vol. 15 (Oxford University Press, 2002).